Synthesis, Characterization, Properties, and Derivatives of Poly(starch-*g*-(1-amidoethylene)). II. Measurement of Molecular Weights by Ultracentrifugation

JOHN J. MEISTER and MU LAN SHA, *Department of Chemistry, University of Detroit, 4001 W. McNichols Rd., Detroit, MI 48221* and E. GLEN RICHARDS, *Research Division, Veterans Administration Hospital, 4500 South Lancaster, Dallas, Texas 75216*

Synopsis

Weight-average molecular weights of samples of poly(starch-*g*-(1-amidoethylene)) determined by ultracentrifugation range from 0.19 to 3.7×10^6. These data show the copolymer to be a partially permeable coil in aqueous solution and to be formed at significantly higher molecular weights as the mole ratio of cerium(+IV) to 2-propenamide in the reaction mixture decreases. Sedimentation coefficients show no indications of distribution broadening from aggregation of copolymer molecules. Buoyancy factor and partial specific volume of the copolymers bracket the values of these variables for the backbone and sidechain.

INTRODUCTION

Molecular weights of polymers can be measured by referenced or absolute methods. Referenced methods such as measurement of limiting viscosity number or use size exclusion chromatography (SEC) often provide quick values of molecular weight. However, for most polymers, the Mark–Houwink constants, K and a, needed to relate molecular weight to limiting viscosity number, $[\eta] = KM_w^a$, are unknown, and, for graft copolymers, these constants would depend not only on molecular weight, but also on the number of grafts attached to the backbone unit of the molecule.[1,2]

SEC separates molecules by size rather than weight and will not give accurate results for grafted copolymers. Grafted macromolecules have a molecular size which is a function of the number of grafts in the molecule as well as total molecular mass.

Of the absolute methods, freezing point depression, ebulliometry, and vapor phase osmometry are all usually restricted to molecular weights below 10^5. Light scattering, while a very versatile method, is difficult to apply to graft copolymers because backbone and side chain often have different indices of refraction. Scattering then depends on molecular composition as well as molecular weight.[3] Membrane osmometry and ultracentrifugation are the only methods which can be used to measure a wide range of graft copolymer molecular weights, and, therefore, the sedimentation velocity method of ultracentrifugation has been used to measure molecular weights on a series of starch-*g*-(1-amidoethylene) copolymers.

Journal of Applied Polymer Science, Vol. 33, 1873–1885 (1987)
 CCC 0021-8995/87/061873-13$04.00

In this paper, a method to measure the sedimentation coefficient s to high accuracy using Rayleigh interference optics is reported. Values and distribution of s, limiting viscosity number, buoyancy factor, molecular weights, and radii of gyration will be given.

EXPERIMENTAL

All solutions used in these tests were made in a solvent of 0.01M Na_2SO_4 in distilled, deionized water. Copolymer was dispersed on a vortex of solvent and then allowed to stir at approximately 60 rpm for a day. This procedure was needed to avoid aggregation of the hydrating copolymer[4] and to allow the copolymer molecules to partially untangle. The double sector interference cell was loaded with 400 L of solvent in one compartment and 400 L of sample in the other. Sedimentation experiments were performed at 44,000 rpm and approximately 20°C. To determine effective time at speed, the rotor was accelerated at constant amperage, and the clock was started at 2/3 of the running speed (29,300 rpm). A "baseline" photo of the cell was taken during a 30 s interval at 5,600 rpm. Photos were then taken at 10–15 min intervals during the run with an exposure time of 8–16 s, depending on arc lamp intensity. The run was continued for a time sufficient to allow sedimentation for smaller polymer molecules. This was determined by visual examination of the pattern to ensure that a "flat" region near the meniscus was present. The positions of the center points for three central fringes in the photographed interference pattern were determined for at least 80 radial positions encompassing the concentration boundary using the profile projector.[5]

Since, by definition

$$s = \frac{1}{\omega^2}\frac{d(\ln r)}{dt} \tag{1}$$

integration from the meniscus, r_0, to a radial distance r along the cell gives the relationship

$$s = \frac{\omega^{-2}\ln(r/r_0)}{t} \tag{2}$$

Equation (2) relates sedimentation coefficients s to a ratio of radial distance along the cell r/r_0 and time t at angular velocity ω. This equation allows position along the cell to be plotted as s instead of r.

At each radial level, the three fringe positions are averaged to give the concentration Y in micrometer units. The number of fringes J seen in the interference pattern is a function of solute concentration c_2, specific refractive increment dn/dc_2, cell thickness along the optical path a, and wavelength of the incident light λ:

$$J = \frac{a(dn/dc_2)c_2}{\lambda} \tag{3}$$

Thus, if Y is the centerpoint of a fringe,

$$J = Y/(\text{fringe separation}) \tag{4}$$

Since fringe units are easily converted to standard concentration units, it is convenient to speak of concentration in terms of the former. Owing to radial dilution of material moving from the meniscus to each radial zone, the concentration profile is corrected according to the standard equation,

$$\Delta J_i = (j_i - j_{i-1}) \times (r_i^2/r_0^2) \tag{5}$$

where J denotes the corrected and j the uncorrected concentrations for the radial interval r_{i-1} to r_i. The corrected concentration profile J is obtained by accumulating $\Sigma\Delta J_i$ to each radial level r_i.

Finally, the data are smoothed and the distribution profile dc/ds is obtained by two passes through a sliding, 15-point cubic least square fit of the J vs. s profile.

Because diffusion is minimal during the short time span of these experiments, the corrected boundary profiles obtained at different times should be identical. Comparison of several patterns for the same experiment provides a measure of the accuracy of the cell geometry, plate measurement, and the data processing. The precision of the fringe measurements was ± 0.01 fringes.

The comparison also allows the Gaussian nature of dc_2/ds to be checked easily and permits checks for warpage of the patterns by such phenomena as the Johnston–Ogston effect.[6]

Solution viscosities were measured at 20°C using a capillary viscometer calibrated with water.[7] Passage times were about 200 s to avoid kinetic energy corrections.[8] Concentration of copolymer ranged up to 1.5 mg/g in steps of 0.25 mg/g. Densities were measured at 20°C in a cold room. Temperature control was ± 0.01°C. Sample was injected into a vibrating tube densitometer, allowed to equilibrate for 10 min, and measured for effect on tube vibration frequency. The device was calibrated with water and air, and all measurements were made in triplicate. Concentrations of polymer in solvent ranged from 2.50 to 0.5 mg/g, usually in 05 mg/g steps.

Equipment

Sedimentation velocity was measured in a Beckman Model E analytical ultracentrifuge using Rayleigh interference optics and a AN-HTI Titanium rotor. A Kel-F centerpiece was used in the 12-mm double-sector cell. Kodak metallographic plates were used to photograph the fringe patterns, with a Kodak Wratten 77A filter to isolate 546 nm mercury green line. The sections were read on a Nikon 6C profile projector with IKL digital micrometers and a Sirco, dual-photocell fringe detector. The reading of data was controlled and stored by an MITS Altair S-100 computer equipped with two Northstar disk drives and floating point board. Computations, fitting, and plotting were done on a Radio Shack Model 3 computer and a Radio Shack plotter.

Viscosities were measured with a Cannon-Fenske #50 viscometer. Densities were measured using a DMAO2C density meter and temperature was controlled using a Haake Type F4391, circulating heater/refrigerator.

Materials

All water used in experiments was distilled and then deionized. Salts, solvents, and gases were all reagent grade and were used as received. Polymer samples were synthesized and characterized as described in Ref. 9. The narrow molecular-weight-distribution poly(1-amidoethylene) used was Polysciences, Inc. #8249, stated to be 500,000 molecular weight material.

RESULTS AND DISCUSSION

To measure sedimentation coefficient for each copolymer, at least four photographs, taken during the ultracentrifugation of a 0.5 mg/mL solution of copolymer in solvent, were measured and analyzed.

One photo, which was always analyzed, was the baseline photograph taken at 5600 rpm. Subtraction of this profile from those data of the other three patterns, all of which were taken at full speed, allowed the data to be corrected for cell window imperfections or equipment effects. The copolymer sedimentation coefficient was calculated as a weight average by integration of the plot of polymer concentration vs. sedimentation coefficient for each analyzed, baseline-corrected photograph.

The sedimentation coefficient from each photograph and average sedimentation coefficient for each copolymer are given in Table I. The standard deviations for the average sedimentation coefficients are of the order of 0.06 for all samples except 9; photo 3 for this sample was not included.

The average sedimentation coefficient increases with increasing design[9] molecular weight, M_{cal}, and decreases with increasing Ce(IV) to starch mole ratio, N_g. These characteristics are described in Ref. 9. Sample 10 is the exception to this pattern and apparently represents an incomplete or defective synthesis.

Sedimentation coefficient for a copolymer is not just a function of copolymer molecular weight distribution,[10] radial dilution in the cell,[11] and solution temperature[12] but also may depend on polymer concentration.[13] To test the dependence of s_w on concentration, a series of sedimentation experi-

TABLE I
Sedimentation Coefficients of Copolymer Samples[a]

Sample number	Photograph 1	Photograph 2	Photograph 3	Average
2	5.05	4.26	4.41	4.57
4	9.86	9.92	9.92	9.90
5	6.31	6.43	6.69	6.48
6	4.88	4.97	5.77	5.21
7	9.77	9.84	9.80	9.80
8	8.10	8.15	8.26	8.17
9	7.24	7.17	12.72	7.21
10	7.00	7.02	7.09	7.04
11	10.8	10.8	10.6	10.7
12	7.64	7.52	7.61	7.54

[a]Weight-average sedimentation coefficient ($s_w \times 10^{13}$) (s).

TABLE II
Sedimentation Coefficient of Poly(1-Amidoethylene) Standard in 1-Day-Old Solutions[a]

Poly(1-amidoethylene) concentration (mg/g)	Photograph			Average
	1	2	3	
0.300	11.2	4.56	3.83	6.54
0.600	10.6	4.22	4.21	6.34
0.900	10.2	4.02	3.95	6.04

[a]Weight-average sedimentation coefficient ($s_w \times 10^{13}$) (s).

TABLE III
Sedimentation Coefficient of Copolymer 9 in 1-Day-Old Solution[a]

Copolymer 9 concentration (mg/g)	Photograph			Average
	1	2	3	
0.25	7.67	8.35	8.46	8.16
0.50	7.25	7.18	12.72	7.21[b]
0.75	6.89	6.77	6.78	6.82
1.00	6.32	6.32	6.46	6.37

[a]Weight-average sedimentation coefficient ($s_w \times 10^{13}$) (s).
[b]Average of photo 1 and 2 values only.

ments was conducted using solutions containing different concentrations of narrow molecular weight poly(1-amidoethylene) standard. Sedimentation coefficients of the polymer at three concentrations are given in Table II. There is a sharp variation in the weight average sedimentation coefficient for this standard. This is thought to be due to entangling in the poly(1-amidoethylene); which is known to disperse slowly to form a monomolecular colloidal solution only after 60 days.[14,15] To determine if the copolymer dispersed rapidly in the solvent and to examine concentration dependence, a series of ultracentrifugation runs were performed on solutions of copolymer 9.

Sedimentation coefficients for copolymer 9 in four solutions ranging in concentration from 0.25 to 1.00 mg/g are given in Table III. The results show that copolymer 9 is a relatively homogeneous dispersion of copolymer molecules in solution after 1 day. The behavior of pure poly(1-amidoethylene), which initially disperses into aggregates containing many molecules and then slowly becomes a monomolecular colloid over a period of days, is not a significant phenomenon in the graft copolymer. The sedimentation coefficient changes with concentration according to

$$s = 8.969\left[1 - \left(3.132 \times 10^{-3} c_2\right)\right] \tag{6}$$

This is the concentration dependence expected for a nonionic polymer.[16] Because of concentration dependence, the weight average molecular weights determined here will be somewhat low.

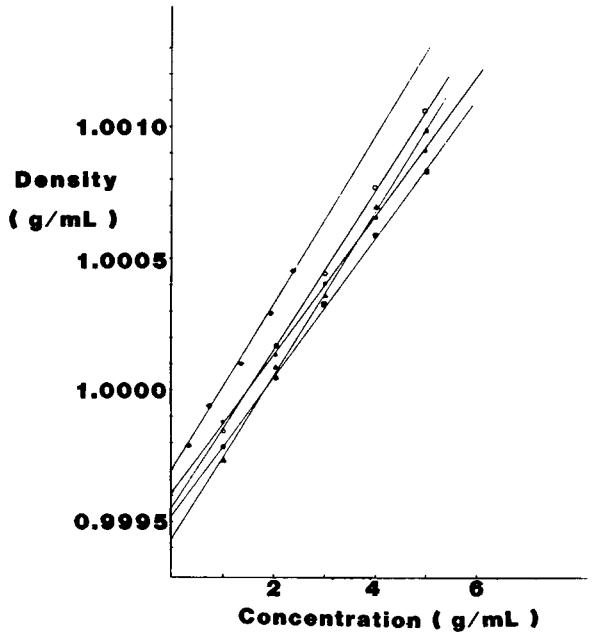

Fig. 1. Representative plots of solution density vs. copolymer concentration for five copolymers: (-●-) sample 4; (▲) sample 5; (○) sample 8; (●) sample 9; (■) sample 7.

The buoyancy factor for each polymer was determined using the method of Eisenburg and Cassassa.[17] Density was measured for each of a series of copolymer solutions of different concentration. The slope of the graph of density versus copolymer concentration is the buoyancy factor.

A representative group of density versus polymer concentration curves are given in Figure 1. Data are highly linear and show an intercept (solvent density) consistent within a relative standard deviation of 0.02%. Buoyancy factor, partial specific volume, and correlation coefficient for a linear fit are given for all polymers in Table IV. Buoyancy factor for poly(1-amidoethylene) was taken from Schwartz et al.[18] Buoyancy factor for starch is within the range commonly reported.[19,20]

Measurements with a capillary viscometer give an average viscosity at a spectrum of shear rates for nonNewtonian fluids. All of the solutions tested are nonNewtonian[21]; however, an average shear rate in the capillary viscometer used is 7 s^{-1} and the shear rate imposed on the copolymer during sedimentation is well below this value. Further, capillary viscosity measurements have a relative precision of 0.14% while fixed-shear-rate measurements of viscosities between 1 and 3 cP are highly imprecise. For these reasons, viscosities from capillary viscometer measurements are used in this work.

Viscosity numbers of a series of copolymer solutions of differing concentration are extrapolated to zero copolymer concentration using the Huggins equation[22]

$$\eta_{sp}/c_2 = [\eta] + Q_H[\eta]^2 c_2 \tag{7}$$

TABLE IV
Buoyancy Factor and Partial Specific Volume of Copolymer

Sample no.	Partial specific volume (cm^3/g)	Buoyancy factor ($1 - \bar{V}\rho$)	Correlation coefficient (%)
2	0.672	0.330	99.9
4	0.639	0.362	99.9
5	0.672	0.329	99.9
6	0.628	0.372	99.9
7	0.712	0.289	99.8
8	0.701	0.300	99.9
9	0.709	0.292	99.7
10	0.596	0.405	99.1
11	0.768	0.233	98.7
12	0.697	0.304	99.9
Starch	0.609	0.392	99.9
Poly (1-amido-ethylene)	0.609	0.293	

TABLE V
Limiting Viscosity Number, Radius or Gyration and Weight-Average Molecular Weight for 10 Copolymers

Sample number	Limiting viscosity number[a] (dL/g)	$\bar{M}_w \times 10^{-3}$	Design molecular weight $\times 10^{-6}$	$(\bar{S}^2)^{1/2}$ ($\times 10^{+6}$ cm)[b]
2	0.621	191	0.2	1.48
4	4.11	1,360	0.4	5.34
5	2.93	701	0.4	3.82
6	1.04	265	0.4	0.92
7	4.96	2,060	0.6	6.53
8	3.16	1,190	0.6	4.67
9	4.63	1,740	0.6	6.03
10	8.69	1,000	0.8	6.19
11	6.42	3,710	0.8	8.66
12	3.68	1,120	0.8	4.82

[a] Measured in distilled water at 20°C.
[b] Hydrodynamic radius of gyration in 0.01*M* $NaSO_4$ solution from eq. (12).

where Q_H is the Huggins coefficient. Correlation coefficient for most fits to eq. (7) is 0.998 or higher. Values for the limiting viscosity number of the tested polymers at 20°C are given in Table V. $[\eta]$ is a function of both the size and shape[23] of the polymer in solution, as well as a function of molecular weight. Shape effects are compensated for in the scaled frictional coefficient

$$\beta = \frac{N^{1/3}}{16{,}200\pi^2}\nu^{1/3}\frac{f_0}{f} \tag{8}$$

where N is Avogradro's number, ν is the viscosity increment,[24] f is the

friction factor, f_0 is the equivalent friction factor of a sphere, and $\beta = 2.16 \times 10^6$.

To facilitate comparison of experimental values of the sedimentation coefficient measured in different solutions or at various temperatures, the results of sedimentation velocity studies are usually converted to a standard basis corresponding to sedimentation coefficient in a reference solvent having the viscosity and density of water at 20°C. The correction of data is accomplished by the method introduced by Svedberg and Pedersen[25] using

$$s_{20,w} = s\frac{(\eta)}{\eta_{20,w}} \times \frac{(1 - \bar{V}\rho)_{20,w}}{(1 - \bar{V}\rho)} \tag{9}$$

Here the term η is the viscosity of the solvent at the temperature of the experiment and $\eta_{20,w}$ is the viscosity of water at 20°C.

Calculation of Molecular Weight

The relationship of sedimentation coefficient $s_{20,w}$, buoyancy factor $(1 - \bar{V}\rho)$, and limiting viscosity number $[\eta]$ to weight-average molecular weight $\bar{M}_w$ is

$$\bar{M}_w = \frac{4690(S_{20,w})^{3/2}[\eta]^{1/2}}{(1 - \bar{V}\rho)^{3/2}} \tag{10}$$

Equation (10) is used to calculate the copolymer molecular weights given in Table V. A plot of these molecular weights versus sedimentation coefficient, as shown in Figure 2, gives the line

$$s_{20,w} = 1.76 \times 10^{-6}(\bar{M}_w)^{1/2} + 5.504 \tag{11}$$

Thus, these copolymers are not free draining coils since the slope in eq. (11) is greater than zero.[26]

Comparison of the measured molecular weights to design molecular weights shows that the actual copolymer molecular weights obtained from synthesis are significantly higher than design. This high molecular weight is caused by several factors. The first is that the property measured is a weight-average molecular weight. This average gives disproportionate emphasis to the higher molecular weight end of the molecular weight distribution. Since poly(1-amidoethylene) is prone to produce such fractions, this will raise the value of $\bar{M}_w$. Second, not all starch molecules are grafted in this reaction.[9] This permits the reacting molecules to grow to chain sizes above the design limit and further increases the high molecular weight end of the distribution. Finally, poly(1-amidoethylene) may terminate by disproportionation[27] or combination[28] (both mechanisms have experimental support). If extensive combination termination occurs, this would sharply increase the high molecular weight end of the distribution.

Since the entire interference pattern of each of three photos of the sedimenting copolymer sample is read, it is possible to obtain a measure of the molecular weight distribution of these copolymers. The number of fringes, J,

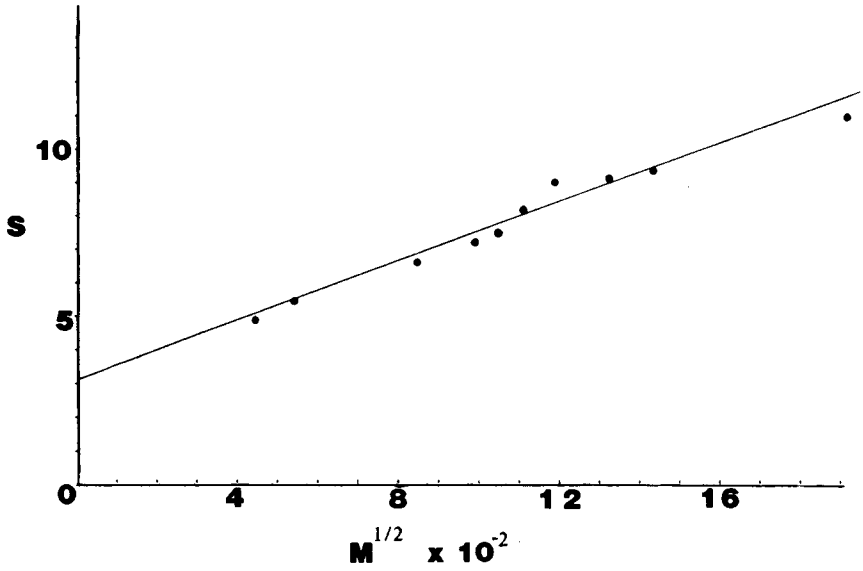

Fig. 2. Test of precision of data by plotting sedimentation coefficient vs. square root of copolymer molecular weight for all samples.

is directly proportional to the concentration of polymer, C_2, and can be summed to get copolymer concentration as a function of sedimentation coefficient plots or fitted as a least-squares function of s to get change of copolymer concentration with respect to sedimentation coefficient vs. s plots. A concentration versus sedimentation coefficient plot for sample 8, photo 1, is given as Figure 3. The derivative plot from this curve, dc_2/ds vs. s, shows

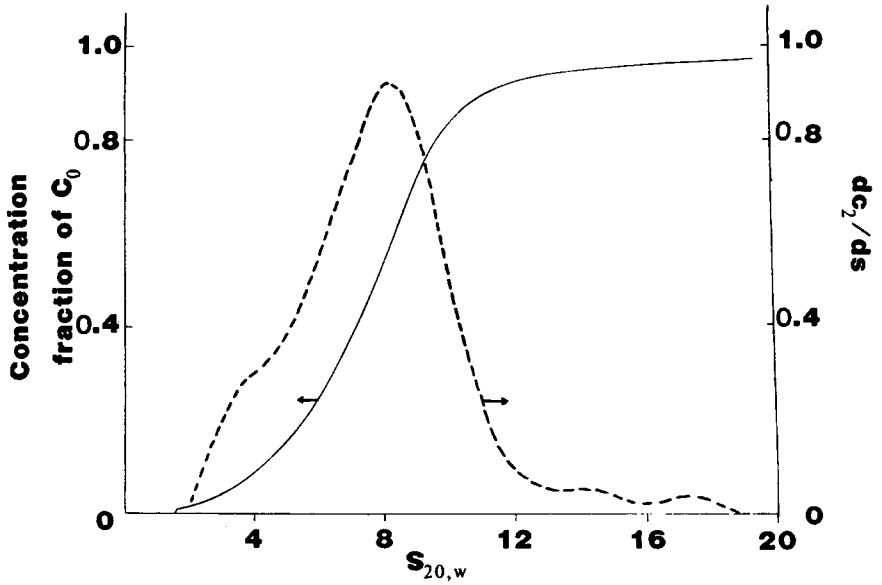

Fig. 3. A plot of copolymer concentration and the derivative of copolymer concentration with respect to sedimentation coefficient vs. sedimentation coefficient calculated from photo 1 of the sedimentation of sample 8.

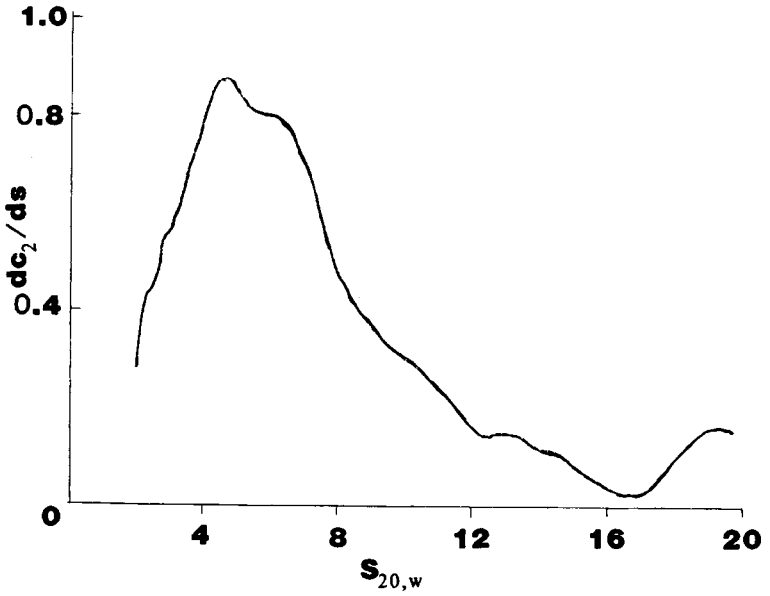

Fig. 4. A plot of the derivative of copolymer concentration with respect to sedimentation coefficient vs. sedimentation coefficient. Data calculated from photo 1 of the sedimentation of sample 6.

that the distribution of molecular weights within the sedimenting copolymer is not normally distributed, but is, instead, skewed to lower s values.

The high concentration of low-sedimentation-coefficient material and the bimodal distribution of molecular size shown in the size exclusion chromatogram for sample 8 show that this sample has a bimodal molecular weight distribution.[9] The most probable cause for this distribution is the presence of a contaminant in the reaction mixture which acted as a chain transfer agent or inhibitor.

Data from ultracentrifugation analysis of sample 6 also indicates a molecular weight variation in the sample. This is clearly seen in the dc_2/ds vs. s curve for sample 6 given in Figure 4. The figure shows that sample 6 also has a skewed molecular weight distribution, but, in this case, the skewing feature is a high molecular weight tail. Samples 6 and 8 also have the highest concentration of insoluble starch of any of the samples. The data of Ref. 9 show that these copolymers are contaminated with 5.6 and 5.5 wt % insoluble starch, respectively. Since the low molecular weight fraction of sample 8 absorbs UV at 210 nm, it contains poly(1-amidoethylene) units.

The causes of the skewed distributions in samples 6 and 8 may be unrelated. However, one factor that could explain the high levels of minimally grafted starch and the skewed molecular weight distributions of these samples is the presence of a chain transfer agent in the reaction vessel.

The dc_2/ds vs. s plot of sample 12 is given in Figure 5 and shows that this sample is contaminated with low molecular weight material. During four syntheses of sample 12, a solid phase formed and increased in volume. This phenomenon was unique to this sample and indicates that reactions with high N_g (cerium ion to starch mole ratio which is 4 for this synthesis) and high D_p

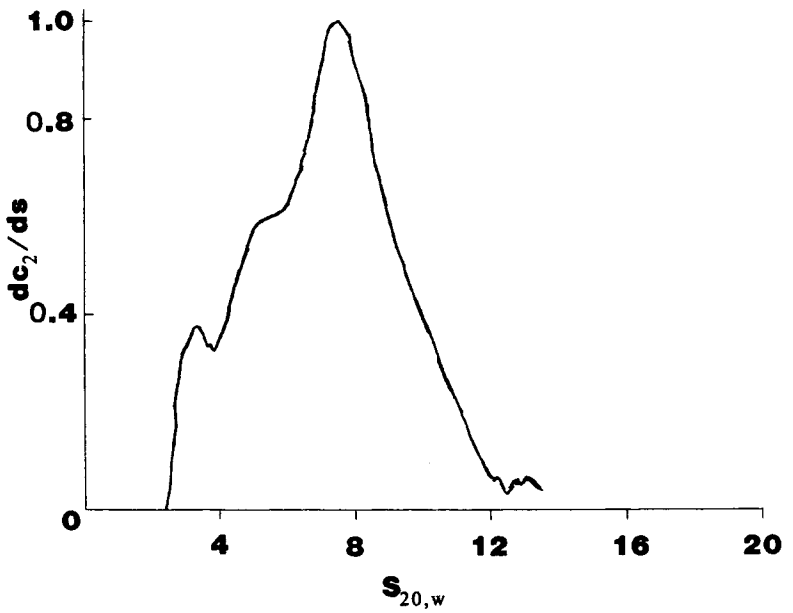

Fig. 5. A plot of the derivative of copolymer concentration with respect to sedimentation coefficient vs. sedimentation coefficient. Data calculated from photo 2 of the sedimentation of sample 12.

(2-propenamide to cerium ion mole ratio) undergo phase separation during synthesis. Since this separation is reproducible, it is not due to a reaction contaminant but is the result of the reactants and the process of this reaction. The skewed molecular weight distribution curve of this graft copolymer may be the result of the precipitation of the high-molecular-weight reaction products of the grafting reaction rather than any reaction process which produces low molecular weight molecules.

Radius of gyration of solvated copolymer $\langle s^2 \rangle^{1/2}$ can be calculated from the Flory equation[22]

$$[\eta] = \frac{\Phi \langle \bar{s}^2 \rangle^{3/2}}{\bar{M}_w} \tag{12}$$

where $\Phi = 2.5 \times 10^{-21}$ mol^{-1} is the broad molecular-weight-distribution, scaling constant. Values of radius of gyration for the ten copolymers characterized are given in Table V. For copolymers designed to have the same number of grafts per starch backbone molecule, radius of gyration increases with increasing molecular weight.

CONCLUSIONS

Weight-average molecular weights of samples of poly(starch-*g*-(1-amidoethylene)) as determined by ultracentrifugation range from 0.19 to 3.7×10^6. These values are greater than the numerical estimates of molecular weight prepared from the composition of the synthesis mixture. This comparison of magnitudes is to be expected since the calculated molecular weight is a

number average and the measured molecular weight is a weight average. These data show the copolymer to be a partially permeable coil in 0.01*M* sodium sulfate and to be formed at significantly higher molecular weight as the mole ratio of cerium(+4) to 2-propenamide in the reaction mixture decreases.

Sedimentation coefficients are precise to 1% and show no indication of distribution broadening because of molecular aggregation. $\bar{s}_w$ determined is concentration-dependent and may be slightly low because of solution concentration effects. $\bar{s}_w$ increases with design molecular weight and decreases with mole ratio of cerium(+4) to starch used in the synthesis mixture. These data are determined from Rayleigh interference images generated by sedimentation velocity experiments and show this technique to be highly effective for determining $\bar{s}_w$ and its distribution.

Buoyancy factors of the copolymers vary from 0.223 to 0.405 and are bracketed by the factors of the two parts, backbone and pure side chain, of the copolymer. Partial specific volumes of the samples vary from 0.596 to 0.768 and are bracketed by the specific volumes of the parts of the copolymer. Limiting viscosity number of the copolymer increases with design molecular weight. Radius of gyration of the solvated copolymer increases with increasing molecular weight when products from reactions with equal synthesis Ce(+4) to starch mole ratio are compared.

Portions of this work were supported by Grant N-834 from the Robert A. Welch Foundation and by the National Science Foundation Grant CBT-8417876. This support is gratefully acknowledged. The aid of George Merriman and Kevin Anderle in measuring some of the limiting viscosity numbers is greatly appreciated.

References

1. B. H. Zimm and W. Stockmayer, *J. Chem. Phys.*, **17**, 1301 (1949).
2. B. H. Zimm and R. W. Kilk, *J. Polym. Sci.*, **37**, 19 (1959).
3. S. Rause, *J. Phys. Chem.*, **65**, 1618 (1961).
4. E. J. Unsal, J. L. Duda, E. E. Klaus, and H. T. Liu, Eastern Regional Conf. Soc. Pet. Eng.–AIME, Paper SPE 6625, Pittsburgh, PA, 1977.
5. E. Glen Richards and J. H. Richards, *Anal. Biochem.*, **62**, 523 (1974).
6. J. P. Johnston and A. G. Ogston, *Trans. Farad. Soc.*, **42**, 789 (1946).
7. J. F. Swindells, J. R. Coe, Jr., and T. B. Godfrey, *J. Res. Natl. Bur. Stand.*, **48**, 1 (1952).
8. S. Oka, in *Rheology*, F. R. Eirich, Ed., Academic, New York, 1960, Vol. 3, p. 17.
9. J. J. Meister and M. L. Sha, *J. Appl. Polym. Sci.*, **33**, 1859 (1987).
10. J. W. Williams, R. L. Baldwin, W. M. Saunders, and P. G. Squire, *J. Am. Chem. Soc.*, **74**, 1542 (1952).
11. T. Svedberg and H. Rinde, *J. Am. Chem. Soc.*, **46**, 2677 (1924).
12. D. F. Waugh and D. A. Yphantis, *Rev. Sci. Instrum.*, **23**, 609 (1952).
13. W. F. Harrington and H. K. Schachman, *J. Am. Chem. Soc.*, **75**, 3533 (1953).
14. N. Narkis and M. Rebhun, *Polymer*, **7**, 507 (1966).
15. W. P. Shyluk and F. S. Stow, Jr., *J. Appl. Polym. Sci.*, **13**, 1023 (1969).
16. J. M. Burgers, *Proc. Acad. Sci., Amsterdam*, **45**, 9, 26 (1942).
17. H. K. Eisenberg and E. F. Casassa, *J. Polym. Sci.*, **49**, 29 (1960).
18. T. Schwartz, J. Francois, and G. Weill, *Polymer*, **21**, 247 (1980).
19. R. Geddes, J. D. Harvey, and P. R. Wills, *Biochem. J.*, **163**, 201 (1976).
20. W. Banks, R. Geddes, C. T. Greenwood, and I. G. Jones, *Staerke*, **24**, 245 (1972).

21. J. J. Meister, G. R. Merriman, and K. C. Anderle, in preparation.
22. M. L. Huggins, *J. Am. Chem. Soc.*, **64**, 2716 (1942).
23. W. R. Moore, in *Progress in Polymer Science*, A. D. Jenkins, Ed., Pergamon, Oxford, 1967, Vol. 1.
24. R. Simha, *J. Phys. Chem.*, **44**, 25 (1940).
25. T. Svedberg and K. O. Pedersen, *The Ultracentrifuge*, Oxford Univ. Press, London and New York, Johnson Reprint Corp., New York, 1940.
26. H. H. Schachman, *Ultracentrifugation in Biochemistry*, Academic, New York, 1959, pp. 245–246.
27. T. J. Suen, Y. Jen, and J. V. Lockwood, *J. Polym. Sci.*, **31**, 481 (1958).
28. J. Francois, D. Sarazin, T. Schwartz, and G. Weill, *Polymer*, **20**, 969 (1979).

Received January 28, 1986
Accepted August 4, 1986